

The Dark Matter Haloes and Host Galaxies of Mg II Absorbers at $z \sim 1$

Britt F. Lundgren¹, David A. Wake¹, Nikhil Padmanabhan¹, Alison Coil^{2,3}, Donald G. York^{4,5}.

¹Yale Center of Astronomy and Astrophysics, Yale University, New Haven, CT 06511, USA

²Department of Physics, University of California at San Diego, San Diego, CA, USA

³Alfred P. Sloan Foundation Fellow

⁴Department of Astronomy and Astrophysics, University of Chicago, Chicago, IL 60637, USA

⁵Enrico Fermi Institute, 5640 Ellis Ave., Chicago, IL 60637, USA

ABSTRACT

Strong foreground absorption features from singly-ionized Magnesium (Mg II) are commonly observed in the spectra of quasars and are presumed to probe a wide range of galactic environments. To date, measurements of the average dark matter halo masses of intervening Mg II absorbers by way of large-scale cross-correlations with luminous galaxies have been limited to $z < 0.7$. In this work we cross-correlate 21 strong ($W_r^{\lambda 2796} \gtrsim 0.6 \text{ \AA}$) Mg II absorption systems detected in quasar spectra from the Sloan Digital Sky Survey Data Release 7 with $\sim 32,000$ spectroscopically confirmed galaxies at $0.7 \leq z \leq 1.45$ from the DEEP2 galaxy redshift survey. We measure dark matter (DM) halo biases of $b_G = 1.44 \pm 0.02$ and $b_A = 1.49 \pm 0.45$ for the DEEP2 galaxies and Mg II absorbers, respectively, indicating that their clustering amplitudes are roughly consistent. Haloes with the bias we measure for the Mg II absorbers have a corresponding mass of $1.8 \pm_{1.6}^{4.2} \times 10^{12} h^{-1} M_\odot$, although the actual mean absorber halo mass will depend on the precise distribution of absorbers within DM haloes. This mass estimate is consistent with observations at $z = 0.6$, suggesting that the halo masses of typical Mg II absorbers do not significantly evolve from $z \sim 1$. We additionally measure the average $W_r^{\lambda 2796} \gtrsim 0.6 \text{ \AA}$ gas covering fraction to be $f_c = 0.5$ within $60 h^{-1} \text{ kpc}$ around the DEEP2 galaxies, and we find an absence of coincident strong Mg II absorption beyond a projected separation of $\sim 40 h^{-1} \text{ kpc}$. Although the star-forming $z > 1$ DEEP2 galaxies are known to exhibit ubiquitous blueshifted Mg II absorption, we find no direct evidence in our small sample linking $W_r^{\lambda 2796} \gtrsim 0.6 \text{ \AA}$ absorbers to galaxies with ongoing star formation.

Key words: quasar absorption lines: general

1 INTRODUCTION

Absorption features in quasar spectra (quasar absorption lines; QALs) provide nearly unbiased probes of the gas and dust content of foreground galaxies and the intergalactic medium (IGM) over vast ranges in redshift. As such, the growing catalogues of QALs now available from large spectroscopic surveys (e.g., SDSS; York et al. 2000) may be used as reliable tracers of the metal abundances of galaxy environments throughout $\sim 90\%$ of cosmic history. However, critical questions regarding the physical origins of QALs remain to be resolved. Metal-rich QALs have a well-established association with $\sim L^*$ galaxies (e.g., Bergeron 1986; Yanny et al. 1987; Cristiani et al. 1987; Bergeron & Boissé 1991; Le Brun et al. 1993; Steidel 1993;

Steidel et al. 1994), but whether the absorbing gas primarily traces the cool extended regions of dark matter haloes, dwarf satellite galaxies, galactic disks, or supernovae-driven outflows remains an active matter of debate.

The root of the ambiguity surrounding the origins of QALs lies in the fact that while these absorbers are easily detected at moderate and high redshifts, where the most prolific UV metal lines (e.g., singly-ionised Magnesium; Mg II, a tracer of photoionised cold gas) are redshifted into the optical, their galactic hosts are nearly always too faint to observe. For a limited number of objects, deep imaging has been used to identify candidate galaxies as hosts of Mg II absorbers (e.g., Le Brun et al. 1993; Steidel et al. 1997; Nestor et al. 2007; Bouché et al. 2007; Straka et al.

2010; Chun et al. 2010; Meiring et al. 2011). The results of these investigations suggest a correlation between absorber equivalent width and host star-formation rate, though many galaxy hosts of large equivalent width absorbers remain undetected in even the deepest imaging.

Recent efforts to determine the typical physical properties of galaxies hosting strong¹ Mg II absorbers have attempted statistical analyses using large absorber catalogues. The typical luminosities and colors of Mg II hosts have been inferred from the stacking of residual light around thousands of quasars exhibiting Mg II absorption (Zibetti et al. 2007; Caler et al. 2010). Host star-formation rates and dust properties have been inferred from spectral stacks of hundreds of identified absorbers (York et al. 2006; Wild et al. 2007; Ménard et al. 2009; Ménard & Chelouche 2009; Ménard et al. 2010; Noterdaeme et al. 2010), and average absorber dark matter halo masses have been indirectly obtained from Mg II clustering measurements (Bouché et al. 2006; Lundgren et al. 2009; Gauthier et al. 2009). The imaging and spectral stacking analyses collectively indicate a general correlation between Mg II equivalent width and the star formation rate of the host galaxy, whilst the clustering analyses suggest a weak global anti-correlation of the absorber equivalent width with galaxy halo mass. Taken together, these findings disfavor the classical picture in which strong Mg II absorption is primarily produced by virialised gas in the extended haloes of massive galaxies.

Now a new paradigm seems to be emerging in which the majority of strong Mg II absorbers originate in galactic disks on scales $<10 h^{-1}$ kpc and in star formation-driven outflows on larger scales, out to ~ 150 kpc. Deep imaging and spectroscopic follow-up of galaxy-absorber pairs at $z > 0.7$ have confirmed the existence of a strong correlation between $W_r^{\lambda 2796} \gtrsim 2\text{\AA}$ absorbers and starburst galaxies (Bouché et al. 2007; Nestor et al. 2010). Further strengthening the case for supernovae-driven outflows is the recent determination that the redshift number density evolution of strong Mg II absorbers traces the global star formation rate (Ménard et al. 2009; Chelouche & Bowen 2010).

However, studies of Mg II absorbers in the local Universe have shown that the origins are less clear in the case of the much larger population of absorbers with $W_r^{\lambda 2796} \lesssim 2\text{\AA}$. In an examination of such lower equivalent width Mg II absorbers at $z \sim 0.2$, Chen et al. (2010) found no compelling evidence of a correlation between absorption properties and the recent star formation histories of galaxies. Furthermore, recent studies of the galactic counterparts of $W_r^{\lambda 2796} \lesssim 2\text{\AA}$ absorbers at $z \sim 0.1$ find no evidence for outflows from star formation (Kacprzak et al. 2011), suggesting that Mg II absorption primarily probes infalling gas from disk/halo processes in normal galaxies, at least for absorbers with similar equivalent widths in the local Universe. To what extent galaxy evolution or galaxy sample selection biases may be able to reconcile the contradictory findings of Mg II origins in star formation-driven outflows at $z \gtrsim 0.5$ and cold mode accretion at $z \lesssim 0.3$ still remains to be determined.

For large data sets, clustering measurements can be used to determine the typical environments of any well-defined sample of extragalactic objects. The space density of strong Mg II absorbers is low – on average, only 0.3 absorbers with $W_r^{\lambda 2796} \gtrsim 0.6\text{\AA}$ are observed per unit redshift along quasar sightlines at $z=0.5$ (Nestor et al. 2005) – so Mg II clustering estimates in the aforementioned works utilised two-point cross-correlations with much more numerous luminous galaxies in order to extract an absorber clustering signal of measurable strength. Luminous red galaxies (LRGs) have thus far been a favored galaxy sample for this purpose, since their observable redshift range in the SDSS has a large overlap with Mg II absorbers. In addition to their convenient redshift range, LRGs are excellent tracers of structure in the Universe (e.g., Eisenstein et al. 2005; Zehavi et al. 2005; Ross et al. 2007; Blake et al. 2008; Wake et al. 2008a), and they exhibit minimal stellar mass evolution over their observable redshift range in the SDSS ($z \lesssim 0.8$) (Wake et al. 2006, 2008a; Brown et al. 2007, 2008; Cool et al. 2008). The dark matter halo bias of LRGs is thus precisely measured (Blake et al. 2008; Wake et al. 2008a; Padmanabhan et al. 2009), making these galaxies a favorable population for amplifying the clustering signals of quasars and absorbers. Measurements of the Mg II-LRG two-point cross-correlation have converged on a typical Mg II dark matter halo mass of $\sim 10^{12} M_\odot$ at $z \sim 0.6$ (Bouché et al. 2004, 2006; Lundgren et al. 2009; Gauthier et al. 2009).

Few deep spectroscopic surveys exist with sufficient numbers of galaxies to attempt measurements of large-scale absorber clustering (and thus, the dark matter bias) at higher redshifts ($z > 0.6$). Lyman break galaxies (LBGs) have been used to examine the bias of strong quasar absorption lines at $z > 2$; Adelberger et al. (2005) measured the clustering of triply-ionised Carbon (C IV) absorption lines ($\lambda\lambda 1548, 1551$) around UV-selected galaxies at $2 < z < 3$ finding that C IV absorbers cluster similarly to typical star-forming galaxies. Still, a similar analysis has not yet been performed for a sample of Mg II absorbers, which trace gas with a lower ionization temperature and are thus not always coincident with C IV absorption.

The DEEP2 Galaxy Redshift Survey (Davis et al. 2003) provides a sample of $\sim 32,000$ galaxies with spectroscopically confirmed redshifts in the range $0.7 < z < 1.45$, ideal for use in correlations with Mg II detected in the SDSS. This galaxy sample is particularly interesting for Mg II investigations, as its star-forming population has been recently found to exhibit ubiquitous Mg II outflows (observed as blueshifted intrinsic absorption in the stacked rest-frame galaxy spectra) across a wide range of galaxy properties (Weiner et al. 2009). The outflows reported for the DEEP2 galaxies have typical column densities of $N_H \sim 10^{20} \text{ cm}^{-2}$ and velocities of $\sim 400 \text{ km s}^{-1}$. These values are consistent with observations from quasar absorption line data, and Weiner et al. (2009) speculate that the ejected gas could eventually reach projected separations of $50 h^{-1} \text{ kpc}$. However, no direct connection between feedback from normal star-forming galaxies and quasar absorption lines has yet been observed.

In this work, we calculate the two-point redshift-space cross-correlation of the full sample of DEEP2 galaxies with 21 Mg II absorbers identified in SDSS DR7 quasar spectra within the DEEP2 survey area. By comparing to the av-

¹ For brevity, throughout this work we will refer to strong absorbers as those with $W_r^{\lambda 2796} \gtrsim 0.6\text{\AA}$, where $W_r^{\lambda 2796}$ is the equivalent width of the 2796Å transition of Mg II in the absorber rest frame.

erage dark matter halo bias of the galaxy sample, obtained through a calculation of the galaxy auto-correlation, we estimate the typical bias of the absorbers and thereby quantify their average halo mass. We also measure the covering fraction of $W_r^{\lambda 2796} \gtrsim 0.6 \text{ \AA}$ absorption for the DEEP2 galaxy sample and compare with previous results. A description of the data is given in Section 2. The methodology we apply for the analysis is described in Section 3, and results are presented in Sections 4-7. A discussion of the results is given in Section 8, and a summary of important findings is presented in Section 9.

Throughout this paper, we assume a flat Λ -dominated CDM cosmology with $\Omega_m = 0.27$, $H_0 = 73 \text{ km s}^{-1} \text{ Mpc}^{-1}$, and $\sigma_8 = 0.8$ unless otherwise stated.

2 DATA

2.1 The Mg II Absorber Sample

The quasar spectra used in this analysis are drawn from the Sloan Digital Sky Survey Seventh Data Release (SDSS DR7 Abazajian et al. 2009). The SDSS DR7 Quasar catalogue (Schneider et al. 2010) contains 88 quasars in regions of overlap with the DEEP2 survey. Each of the quasars in the DEEP2 survey area was run through an automated pipeline that detects strong Mg II absorption systems with high precision (for full description, see York et al. 2011). In brief, this pipeline first searches for absorption features in quasar spectra. For each detected absorption feature, a Gaussian profile is fit to the normalised flux to extract precise centroid and equivalent width measurements. In order to identify the ion and redshift corresponding to each measured absorption line, a system-finding algorithm then identifies pairs of 4σ absorber detections matching the wavelength separation expected for Mg II at a given redshift. The reliability of the identification is further quantified for each detected absorption system, taking into account the doublet ratio measured for Mg II, the number of additional ions matched in absorption at the same redshift, and any blending with other absorption features identified at another redshift.

Due to the magnitude-limited design of the SDSS survey, the spectral signal-to-noise ratio (SNR) correlates with the optical apparent magnitude of each quasar. The completeness of the SDSS absorption line data for any object thereby varies simultaneously with absorber equivalent width and quasar magnitude, such that the fainter the quasar, the poorer the spectral SNR, and thus the larger the minimum absorber equivalent width for detection at the required 4σ limit. A full description of the detection completeness is provided in York et al. (2011), but generally $z \sim 1$ Mg II absorption systems with $W_r^{\lambda 2796} > 0.6 \text{ \AA}$ are detected with $> 90\%$ completeness in SDSS quasars with $m_i \leq 20$. Because we include in our sample quasars with $m_i > 20$, all candidate absorption systems were verified by visual inspection to rule out any false detections due to artifacts such as problematic continuum subtraction around narrow emission lines or noise spikes.

In all, we find 21 Mg II absorption systems with $W_r^{\lambda 2796} \geq 0.6 \text{ \AA}$ and a velocity separation of $v > 15,000 \text{ km s}^{-1}$ in the quasar rest frame. This velocity difference is generally sufficient to ensure that the absorbers are unambiguously

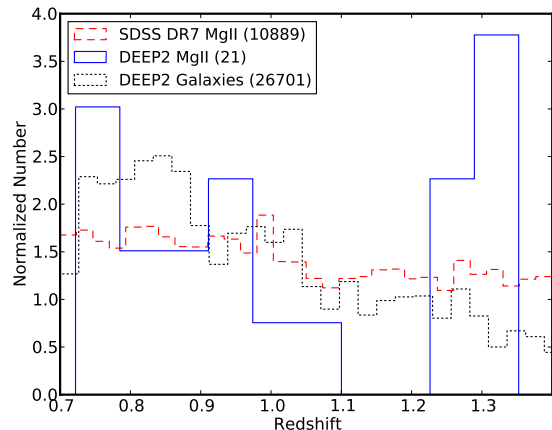


Figure 1. The normalised redshift distributions of the 21 Mg II absorbers and 26,701 DEEP2 galaxies examined in this work. We also include the redshift distribution of all $\sim 11,000$ Mg II absorbers detected over the redshift range of interest in the SDSS DR7 (York et al. 2011), indicating that our data is consistent with a random sample of the global population. The effects of differences in these redshift distributions on the calculation of the Mg II-galaxy cross-correlation have been measured and are discussed in Section 4.

unassociated with the background quasar and thus originating in foreground galactic environments (Wild et al. 2008). The mean rest-frame equivalent width of the 18 absorbers extracted from spectra with $m_i \leq 20$ is $\langle W_r^{\lambda 2796} \rangle = 1.19 \text{ \AA}$, compared to $\langle W_r^{\lambda 2796} \rangle = 1.88 \text{ \AA}$ for the remaining 3 absorbers drawn from fainter quasars. While we expect that the three included spectra with $m_i > 20$ are only complete to $W_r^{\lambda 2796} = 1.0 \text{ \AA}$, these data represent a small fraction of the selected sample. Additional details of the Mg II absorber detections are provided in Table 1.

2.2 The DEEP2 Galaxy Sample

The galaxies used in this analysis are taken from the DEEP2 Galaxy Redshift Survey (Davis et al. 2003), which obtained spectra for $\sim 32,000$ galaxies using the DEIMOS spectrograph (Faber et al. 2003) on the Keck II telescope. The DEEP2 survey observed galaxies in the redshift range $0.7 < z < 1.45$, with a limiting magnitude of $R_{AB} = 24.1$. A magnitude cut of $18.5 < R_{AB} < 24.1$, in combination with a BRI color cut, was applied to select galaxies in the redshift range of interest from CFHT CFH12K imaging (Coil et al. 2004b). The survey geometry consists of four spatially separated fields, which together cover 3 deg^2 of the sky. Additional details of the survey observations and data reduction are available in Davis et al. (2003), and Coil et al. (2004a). The DEEP2 galaxy catalog is a flux-limited sample with $\langle m_R \rangle = 23.3$ and a mean rest-frame B-band luminosity $\langle M_B \rangle = -20.1$, which has been used extensively for clustering measurements at $z \sim 1$. For this work, we apply the exact sample used by Coil et al. (2007) to measure the quasar-galaxy cross-correlation.

3 THE TWO-POINT CROSS-CORRELATION FUNCTION

Due to the extremely low space density of the Mg II systems in our sample, we are unable to measure the absorber clustering by way of an auto-correlation function. However, we can exploit the high space density of the DEEP2 galaxies to measure the clustering of the Mg II systems via their cross-correlation with these galaxies.

The two-point cross-correlation function between two sets of objects a and b , $\xi_{ab}(s)$, is defined as a measurement of the excess probability above Poisson of finding an object a at a separation s from another object b . In order to calculate the Mg II-galaxy two-point correlation function, we compare the number of Mg II-galaxy pairs to the number of Mg II-random pairs as a function of scale such that,

$$\xi(s) = \frac{n_R N_{AG}(s)}{n_G N_{AR}(s)} - 1, \quad (1)$$

where N_{AG} and N_{AR} are the absorber-galaxy and absorber-random pair counts respectively, n_G and n_R are the number of DEEP2 galaxies and DEEP2 random galaxies respectively, and s is the pair separation in redshift space. We choose to use this estimator for the cross-correlation since it only requires a random catalogue for the galaxies, and hence only knowledge of the galaxy selection function is required. This greatly simplifies our calculation, since the selection function of the Mg II absorbers is complex.

The DEEP2 random galaxy catalogue is generated following the spatially dependent selection function of the DEEP2 galaxies, which takes into account the window function of the survey and the spatially dependent redshift success rate, along with the redshift selection function. Details of this procedure are given in Coil et al. (2007). We generate a random catalogue that is 1000 times larger than the galaxy catalogue, which is sufficient to ensure shot noise in the absorber-random pair counts does not contribute significantly to our error budget.

We generate errors on the cross-correlation by bootstrap resampling the absorber systems. We draw 1000 randomly selected samples of 21 absorbers including repeats and recalculate the cross-correlation function. We then find the central 68% of these measurements to define the 1σ error on each point. Normally such a technique would be unsuitable for a clustering measurement, but the absorbers are so spatially sparse that they are essentially independent of each other.

Since the cross-correlation function is related to the auto-correlation functions of both input samples, we need to measure the auto-correlation of the DEEP2 galaxies in order to determine the clustering properties of the Mg II absorbers. For this measurement we use the Landy & Szalay (1993) estimator as:

$$\xi(s) = \frac{N_{GG}(s) - 2N_{GR}(s) + N_{RR}(s)}{N_{RR}(s)} - 1, \quad (2)$$

where N_{GG} , N_{GR} , and N_{RR} respectively represent the galaxy-galaxy, galaxy-random, and random-random pair counts. This slightly more complex estimator differs from what was used to calculate the absorber-galaxy cross-correlation; however, we repeated the calculation of the galaxy auto-correlation using an estimator symmetric to Eq. 1 and found no significant difference in the results.

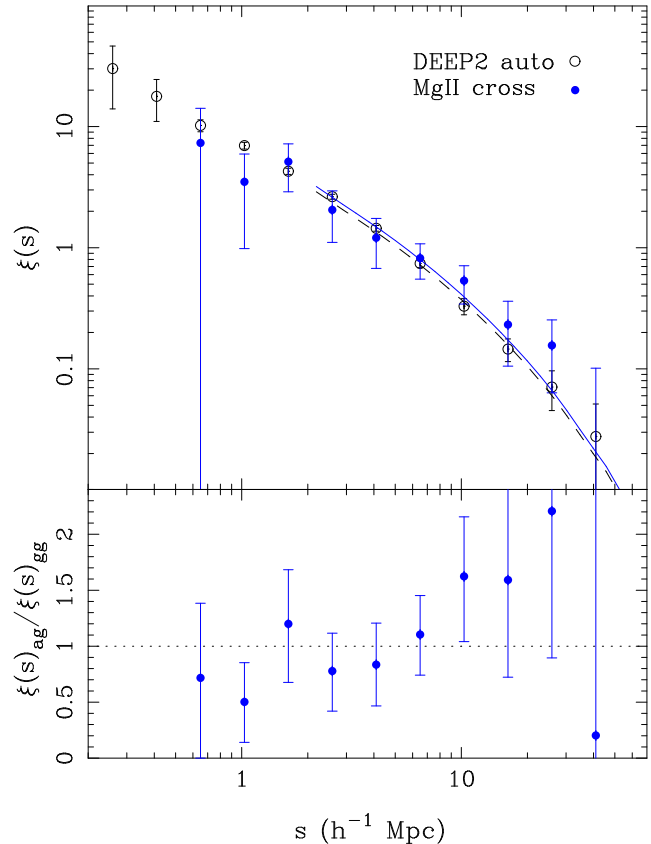


Figure 2. The two-point redshift-space cross-correlation of Mg II absorption line systems and DEEP2 galaxies is shown in comparison with the auto-correlation of the same DEEP2 galaxies, each with 1σ confidence intervals overplotted. The galaxy auto-correlation and absorber-galaxy cross-correlation are consistent within each other on all scales suggesting that the absorbers occupy the same average environments as the DEEP2 galaxies.

We use the same randoms as before but this time estimate the errors using jackknife resampling, removing each of the 10 DEEP2 DEIMOS fields, one at a time. Whilst one would normally need more than 10 fields to accurately estimate the errors and covariance of a clustering measurement using this technique, our overall error budget is dominated by the errors on the cross-correlation. We thereby find this small number of fields to be sufficient for our purposes.

We show in Figure 2 the redshift space Mg II absorber-DEEP2 galaxy two-point cross-correlation function (filled circles) compared to the two point auto-correlation of the galaxies (open circles). Within the errors the Mg II-galaxy cross-correlation and the galaxy auto-correlation are indistinguishable, implying that on scales larger than $0.6 h^{-1}$ Mpc Mg II absorbers live in the same environments as the DEEP2 galaxies.

4 THE BIAS AND DARK MATTER HALO MASSES OF MG II ABSORBERS

The relationship between the clustering of galaxies and the clustering of the underlying dark matter distribution is often described by the bias (b) parameter. In the simplest case the bias (b) is just assumed to be independent of scale so that

$\xi_{gal}(r) = b^2 \xi_{DM}(r)$ and so it is straightforward to estimate b if $\xi_{DM}(r)$ is known.

In our case we have measured the redshift space correlation function, $\xi(s)$, rather than the real space correlation function, $\xi(r)$, and so must take into account the effect that the peculiar velocities of galaxies have on the distance measurements in the redshift direction. There are two terms that contribute to the peculiar velocity: the small scale random motion of galaxies with DM haloes and the large scale coherent streaming of galaxies from underdense to overdense regions, known as the Kaiser effect (Kaiser 1987). Since we only wish to measure the bias we can restrict ourselves to consider only the large scale clustering amplitude which means we only include the Kaiser effect when converting from $\xi(r)$ to $\xi(s)$.

Kaiser (1987) showed that one can relate $\xi(s)$ to $\xi(r)$ as

$$\xi(s) = \xi(r) \left(1 + \frac{2}{3}\beta + \frac{1}{5}\beta^2 \right), \quad (3)$$

where

$$\beta \simeq \frac{\Omega_m^{0.55}}{b} \quad (4)$$

and Ω_m is the matter density of universe at the redshift of interest.

On large scales the cross-correlation can be determined from the respective auto-correlations with $\xi_{AG}^2 = \xi_A \xi_G$, and it is related to the dark matter clustering as $\xi_{AG}(r) = b_A b_G \xi_{DM}(r)$. Therefore the conversion from real space to redshift space must include β terms for both the absorbers and the galaxies and may be parameterised as

$$\xi_{AG}(s) = \xi_{AG}(r) \left[1 + \frac{1}{3}(\beta_A + \beta_G) + \frac{1}{5}\beta_A \beta_G \right] \quad (5)$$

where β_G and β_A depend on the bias of the galaxies and absorbers, respectively.

We calculate $\xi_{DM}(r)$ at $z = 0.95$, the mean galaxy redshift, as described in Wake et al. (2011) using the non-linear power-spectrum produced by the CAMB package² which makes use of the HALOFIT routine from Smith et al. (2003). We then measure the DEEP2 galaxy bias by fitting to the galaxy auto-correlation function. Fitting on large scales allows us to include the value of the galaxy bias in Equation 5 and fit to the Mg II-DEEP2 cross-correlation to extract the absorber bias. Estimates of the scales at which $\xi(s)/\xi(r)$ reach the linear theory asymptote (i.e. there is no effect from peculiar velocities and only the Kaiser (1987) corrections need to be applied) range from 4-8 h^{-1} Mpc (Hawkins et al. 2003; Tinker et al. 2006). We choose to make two fits on scales $> 2h^{-1}$ Mpc and $> 6h^{-1}$ Mpc. The smaller scale yields a higher signal-to-noise measurement but may be biased due to any difference in the peculiar velocities of absorbers and galaxies resulting in a difference in the suppression of $\xi(s)$. Any such bias is likely to be dwarfed by our measurement errors and indeed both fits are equivalent within the errors. It would of course be possible to overcome these potential biases by using the projected correlation function, but with such low numbers of absorbers the measurement becomes incredibly noisy and essentially unusable.

In order to estimate the errors on the measured cross-correlation we fit to each of our bootstrap samples and again find the central 68th percentile to represent the 1σ error. This yields bias measurements for the DEEP2 galaxies of 1.44 ± 0.02 ($s > 2h^{-1}$ Mpc) and 1.38 ± 0.05 ($s > 6h^{-1}$ Mpc) and bias measurements of 1.49 ± 0.45 ($s > 2h^{-1}$ Mpc) and 1.92 ± 0.61 ($s > 6h^{-1}$ Mpc) for the Mg II absorbers. We note that not incorporating the Kaiser effect in our modeling of the measurements produces bias values that are 20% higher.

We can use these bias measurements to estimate the halo mass of both the absorbers and galaxies. The simplest approach is to determine which mass halos have the same bias as the absorbers or galaxies using the halo mass bias relation of Tinker et al. (2010). By this method, we calculate mean halo masses of $\langle \log M \rangle = 12.19 \pm 0.03 M_\odot$ ($s > 2h^{-1}$ Mpc) and $\langle \log M \rangle = 12.09 \pm 0.08 M_\odot$ ($s > 6h^{-1}$ Mpc) for the DEEP2 galaxies and $\langle \log M \rangle = 12.25 \pm_{0.95}^{0.52} M_\odot$ ($s > 2h^{-1}$ Mpc) and $\langle \log M \rangle = 12.74 \pm_{0.71}^{0.46} M_\odot$ ($s > 6h^{-1}$ Mpc) for the Mg II absorbers.

However, we know that the galaxies and absorbers will not occupy haloes of a single mass in this manner but will be distributed over a range of halo masses. This distribution is known as the halo occupation distribution (HOD). There are many different HODs that can yield the same value of the bias, for instance adding more high mass haloes can be balanced out with more low mass haloes. However, since the relationship between bias and halo mass is non-linear these different HODs can yield different mean halo masses for the same bias. Therefore, if we wish to estimate an accurate mean halo mass it is important to use the appropriate HOD.

Much work has been done on determining the HOD for galaxy samples and a suitable form for luminosity limited samples is given by Zheng et al. (2005) (approximately a step function for central galaxies and a powerlaw for satellites). While our galaxy sample isn't strictly luminosity limited it should yield a reasonable estimate of the mean halo mass (see Appendix A of Wake et al. 2008). If we fit using this HOD with parameters suitable for the DEEP2 galaxies and a halo model as described in Wake et al. (2011) we find a higher mean halo mass of $\langle \log M \rangle = 12.63 \pm 0.01 M_\odot$. The same formalism may be applied to the Mg II absorbers, yielding a mean halo mass of $\langle \log M \rangle = 12.66 \pm_{0.15}^{0.11} M_\odot$.

However, there is no reason to believe that Mg II absorbers have a HOD that resembles a luminosity limited galaxy sample. Whilst the gas causing the absorption is likely to trace the underlying galaxy population its presence or absence will depend on additional physics, such as gas temperature, that will be correlated with the dark matter halo properties in a complex way (see Tinker & Chen (2008) for a Mg II-specific HOD model). With a significantly more precise measurement of the Mg II absorber-galaxy cross-correlation it will be possible to put constraints on the Mg II absorber HOD. Such a measurement requires a larger overlapping survey, so we must reserve this analysis for future work.

One possible systematic error that could affect the bias and halo mass determinations arises if the galaxy and absorber samples have different redshift distributions and the galaxy clustering amplitude, and hence bias, depends on redshift. We show in Figure 1 the redshift distribution of the DEEP2 galaxies, the full DR7 Mg II absorber catalogue and the 21 Mg II absorbers in the DEEP2 area. The full DR7

² <http://camb.info>

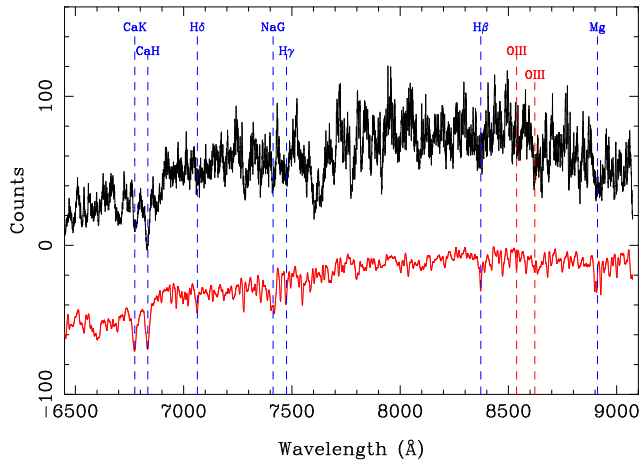


Figure 3. The spectrum of galaxy DEEP2 41013534, with $z=0.72218$, shown in black with a 12 pixel FWHM Gaussian smoothing. The flux is uncalibrated and given in units of DEIMOS counts per hour. The locations of specific absorption features in the galaxy are labeled in blue, and the locations of expected OIII emission are shown in red along with an example template of a 4 Gyr old single age stellar population (also shown in red). This object has the smallest projected physical separation with a Mg II absorber in our sample ($\rho_{gal}=37 \text{ h}^{-1} \text{ kpc}$), which has $W_r^{\lambda 2796}=1.78 \text{ Å}$ and $z_{abs}=0.72191$.

Mg II sample is fairly flat with redshift and so would trace the DEEP2 sample evenly, however the Mg II absorbers in the DEEP2 area have a clear structure in their redshift distribution, which could potentially bias our calculations.

Since the DEEP2 galaxy sample is magnitude-limited, the clustering amplitude we measure could contain a redshift-dependent bias due to the preference for detecting more luminous (and thus more biased) galaxies at higher redshifts. However, Coil et al. (2007) find no significant effect on the relevant scales and we again confirm this with our calculations. We do see a trend on small scales ($< 1 h^{-1} \text{ Mpc}$) and some variation on the largest scales ($> 20 h^{-1} \text{ Mpc}$), although this could well be caused by measurement error.

To test to what extent redshift-dependent bias affects our measurements, we select a sample of DEEP2 galaxies that match the redshift distribution of the 21 Mg II absorbers in DEEP2 area. We do this by selecting the 60 DEEP2 galaxies that have redshifts closest to the redshift of each absorber yielding a sample of 1260 galaxies. We then cross-correlate these galaxies with the full DEEP2 sample and find a cross-correlation function almost identical to the auto-correlation of the full sample (weighted mean difference $< 1\%$ for $0.2 < s < 40$). This result indicates that the differing redshift distributions should have no effect on our results.

5 THE GALAXY PROPERTIES OF SMALL-SCALE PAIRS

Whilst the two-point cross-correlation analysis provides us with information about the distribution of Mg II absorbers relative to massive galaxies on large scales, the detection of prominent Mg II outflows in the spectra of the star-forming

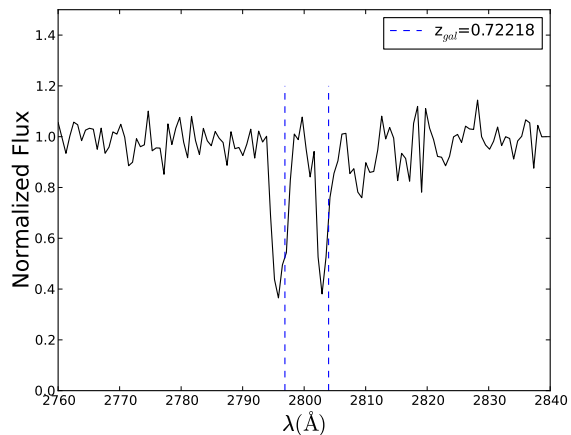


Figure 4. The corresponding detection of a Mg II doublet in close proximity to the galaxy DEEP2 41013534, plotted in Figure 3. The normalised and continuum-subtracted spectrum of quasar SDSS J022800.64+002711.6 is shown in the rest frame of detected absorption: $z_{abs}=0.72191$. The expected location of each transition of Mg II at the redshift of the nearby galaxy ($z_{gal}=0.72218$) is overplotted with a blue dashed line. The difference in their positions corresponds to a velocity offset of 47 km s^{-1} .

$z \sim 1.4$ DEEP2 galaxies reported by Weiner et al. (2009) suggests that, given a sufficient number of close quasar sightlines, one might find frequent absorption coincident with these galaxies on small scales. Adding to this expectation is the observational data indicating that L^* galaxies typically have a cold gas covering fraction of unity on scales less than $60 \text{ h}^{-1} \text{ kpc}$ (Bergeron & Boissé 1991; Bechtold & Ellingson 1992; Steidel et al. 1994).

Three galaxies in the DEEP2 spectroscopic sample are located within $60 \text{ h}^{-1} \text{ kpc}$ of quasar sightline in the SDSS DR7. These galaxies have DEEP2 DR3 catalogue IDs of 31052516, 41013534, 41045894 and respective redshifts of 0.7346, 0.7222, and 0.8488. The first two of the three neighboring quasar spectra exhibit Mg II absorption that is sufficiently strong so as to be identified by the automated pipeline. These detected absorbers have redshifts of 0.7459 and 0.7219 (see ID numbers 15 and 16 in Table 1). The third quasar spectrum has sufficient signal-to-noise such that we would expect to detect an absorber with the minimum equivalent width of our sample, should it be present. However, we detect no Mg II absorption of this strength in the spectrum.

The Mg II absorber with $z=0.7219$, which has the smallest measured projected comoving separation from any DEEP2 galaxy ($37 \text{ h}^{-1} \text{ kpc}$), exhibits an equivalent width of 1.78 Å , which is slightly greater than the mean value for our sample (1.29 Å). The velocity offset between the galaxy and the detected absorption is well within the 3σ confidence intervals for the DEEP2 galaxy redshifts, making this pair a likely direct detection of both absorber and host galaxy. The DEEP2 spectrum of the galaxy in this close pair is shown in Figure 3, and the corresponding Mg II detection is presented in Figure 4.

While the spectroscopically identified galaxy DEEP2 41013534 has the smallest angular separation from this quasar sightline, eight other likely galaxies are identified in the DEEP2 photometric catalogue within $100 \text{ h}^{-1} \text{ kpc}$ of the

same absorber, and three of these are detected within a projected separation of $60 \text{ h}^{-1} \text{ kpc}$. Due to the detection of more than one object within this radius, we cannot say with complete certainty that the spectroscopically observed galaxy is singly related to this Mg II absorber. However, the nearly exact match in redshift and small projected separation makes a strong argument for a physical link between the spectroscopic galaxy and absorption complex.

If we assume that this absorber and galaxy are associated, the physical characteristics of the galaxy spectrum can provide insight into the origin of the strong Mg II absorption complex. The spectrum of galaxy DEEP2 41013534 exhibits typical early-type characteristics. We find no observable emission lines in this spectrum that may be attributed to active star formation. Additionally, the rest frame U-B color of this galaxy is 1.5, placing it firmly on the red sequence. Due to the redshift of this galaxy and the spectral coverage of the DEEP2 survey, we are unable to determine whether this galaxy exhibits evidence of intrinsic, blue-shifted Mg II absorption, which has been observed in many star-forming DEEP2 galaxies (Weiner et al. 2009). However, the absence of any other clear star-formation indicators in this galaxy implies that we cannot directly link the strong coincident Mg II absorption with a measurable rate of ongoing star formation activity in this case.

If we consider a scenario in which the Mg II absorbing gas originated in this galaxy during an earlier period of star formation activity, we can roughly constrain the time since the original burst. Assuming that it is emitted isotropically, gas with an outflow velocity of 400 km s^{-1} , which is typical for the star-forming galaxies measured by Weiner et al. (2009), would take $\sim 100 \text{ Myr}$ to travel the comoving distance of $37 \text{ h}^{-1} \text{ kpc}$ to the quasar sightline. Stellar absorption features in the stacked spectra of similar quiescent galaxies in DEEP2 with $0.7 \lesssim z \lesssim 1$ indicate that these galaxies have an average age of $\sim 1 \text{ Gyr}$ (Schiavon et al. 2006). Considering that we are unable to constrain the specific velocity of outflows from such a star formation event in this galaxy, the estimated age of the galaxy appears to be roughly consistent with the time required for the gas to reach the separation at which it is observed. So, while we are unable to directly connect the observed Mg II absorption in this close pair to ongoing star formation, we also cannot rule out a scenario in which the gas was emitted during an earlier period of star formation activity $\sim 1 \text{ Gyr}$ in the past.

We emphasize that this single absorber-galaxy pair is a perilously small sample from which to draw conclusions regarding the average star-formation properties of Mg II host galaxies. However, given the growing collection of literature linking strong Mg II absorbers with active star formation, particularly at higher redshifts, we found the contradiction presented by this absorber-galaxy pair to be at least somewhat provocative and worthy of discussion.

6 THE MG II COVERING FRACTION OF DEEP2 GALAXIES

The incidence of Mg II absorption in close proximity to galaxies provides an estimate of the cold gas covering fraction, f_c , of galaxy haloes. Measurements of f_c determined for a range of comoving separations allow us to constrain the

effective gas radius, R_g , which is critical for understanding the gas physics in galaxy evolution as well as for properly parameterizing hydrodynamic simulations.

Among the full galaxy sample of DEEP2, 63 galaxies are detected within a projected distance of $200 \text{ h}^{-1} \text{ kpc}$ from a SDSS quasar sightline in which Mg II at the redshift of the galaxy would be observable outside of the Lyman- α forest. If we restrict this number to quasars having observed magnitudes of $m_i \lesssim 20$, the approximate SNR limit to which we can reliably detect Mg II with $W_r^{\lambda 2796} \gtrsim 0.6 \text{ \AA}$ at the median redshift of our sample, 41 galaxies remain. For each included quasar-galaxy pair we search for Mg II in our list of 21 absorbers presented in Table 1. Allowing for a redshift separation of $|z_{gal} - z_{abs}| < 0.008$, we count the number of absorber-galaxy pairs and compare to the total number of observable quasar-galaxy pairs available in order to compute f_c as a function of impact parameter in the rest frame of the absorbers. The width of the redshift bin in this calculation is equivalent to the scale of the maximum outflow velocities detected in Weiner et al. (2009) (1000 km s^{-1}) at the maximum redshift of galaxies in DEEP2, $z=1.4$.

We measure the $W_r^{\lambda 2796} \gtrsim 0.6 \text{ \AA}$ Mg II covering fraction for DEEP2 galaxies to be $f_c=0.5$ (1 detected absorber in a sample of 2 quasar-galaxy pairs) on scales of $20\text{--}60 \text{ h}^{-1} \text{ kpc}$, which decreases rapidly with increasing impact parameter. In the range $20\text{--}100 \text{ h}^{-1} \text{ kpc}$, we find a covering fraction of $f_c=0.125 \pm 0.17_{-0.103}^{+0.17}$ (1 absorber detected among 8 possible quasar-galaxy pairs), and between 100 and $200 \text{ h}^{-1} \text{ kpc}$, f_c drops to zero (measured from a sample of 33 possible quasar-galaxy pairs). Due to the small size of our statistical sample, we estimate the 1σ errors on these measurements using the prescriptions of Helene (1984), which assumes data with a Poisson distribution.

It is important to emphasize that our covering fraction estimates are driven by the detection of the single absorber, which is discussed in the previous section. Because we do not detect any galaxy-absorber pairs with larger projected separations, it is fair to speculate that the typical effective gas radius of the DEEP2 sample may be as small as $\sim 40 \text{ h}^{-1} \text{ kpc}$. The sample we examine is, however, undesirably small and limited by our conservative cuts on the SNR of the SDSS quasar spectra.

7 COMPLETENESS OF THE GALAXY AND ABSORBER SAMPLES ON SMALL SCALES

The obscuration of foreground galaxies by the brighter background quasar is commonly evoked to explain the lack of detected absorber-galaxy pairs with small angular separations. Investigating the angular incidence of DEEP2 galaxies around SDSS quasars with detected absorption, we found no galaxies within $2.8''$ (equivalent to a comoving distance of $30 \text{ h}^{-1} \text{ kpc}$ at $z=1$). This finding indicates that the photometric DEEP2 catalogues are incomplete on scales smaller than this separation around the quasars we examine. At slightly larger radii we find no evidence for photometric objects being systematically excluded for spectroscopic follow-up, so we expect our analysis to be complete beyond this radius.

In addition to this photometric incompleteness, our analysis may also be limited by the spectroscopic resolution of the data. The galaxy redshifts in the DEEP2 catalogue

have a typical 1σ precision of $\sigma_z = 1.3 \times 10^{-4}$ which corresponds a physical scale of $\sim 400 \text{ h}^{-1} \text{ kpc}$ for matter in the Hubble flow at $z=1$. As such, detections of galaxies and absorbers that are physically associated at the same redshift may still have measured separations on the order of this limiting resolution.

To investigate any possible incompleteness in the Mg II data, we re-examined the spectra of all quasars with a projected separation of $< 200 \text{ h}^{-1} \text{ kpc}$ from DEEP2 galaxies. Stacking each of these 63 spectra in the rest-frame of the nearby galaxy revealed a 2σ cumulative detection of Mg II, which grew in significance as we reduced the maximum projected separation allowed. After examining the individual spectra contributing to the stack, we determined that no Mg II absorbers with $> 3\sigma$ significance were undetected by the automated algorithm. We also found that the bulk of the contribution to the Mg II absorption signal in the stacked spectrum could be attributed to the single, strong Mg II absorber with a $37 \text{ h}^{-1} \text{ kpc}$ separation from a DEEP2 galaxy (ID 16 in Table 1), which has been thoroughly discussed in Section 5.

8 DISCUSSION

The bias we measure for Mg II absorbers is consistent with that of the DEEP2 galaxies, although the measurement error is substantial due to the small size of the Mg II sample. This basic agreement suggests that strong Mg II absorbers at $z \sim 1$ reside in similar environments to those of the galaxies in the DEEP2 survey.

Furthermore, the average Mg II halo mass we estimate, $1.56 \pm 0.11 \times 10^{12} M_\odot$, is consistent with observations at lower redshift. Lundgren et al. (2009) measured a typical halo mass of $1.8 \pm_{1.6}^{4.2} \times 10^{12} h^{-1} M_\odot$ for absorbers with $W_r^{\lambda 2796}$ at $z=0.6$, in agreement with Bouché et al. (2006) and Gauthier et al. (2009). The consistency with our measurement at higher redshift suggests that the halo masses of Mg II absorbers evolve very little from $z=1$, though the errors remain large.

It is also worth noting that the luminosity function of $z \sim 0.65$ galaxies selected by Mg II absorption in nearby quasar sightlines has been shown to peak at $M_B = -20$ (Steidel et al. 1994), which is consistent with the mean luminosity of the DEEP2 galaxies. While we have not analysed a statistical sample of Mg II-selected galaxies, it seems likely that the $z \sim 1$ Mg II absorbers not only trace the same environments as the DEEP2 galaxy sample but also similar types of galaxies ($\sim L_B^*$).

8.1 Constraining Mg II Halo Evolution

As measurements of the bias of Mg II have never been reported at this redshift, we can provide the first constraints on theoretical models describing the evolution of absorbers and their respective haloes. Tinker & Chen (2008) produced a model for the halo occupation distribution of cold gas at $z=0.6$, where the bias of Mg II has been precisely measured from cross-correlations with LRGs. With this model, Tinker & Chen (2008) predict the probability of finding an absorber with an equivalent width W_r in a halo of mass

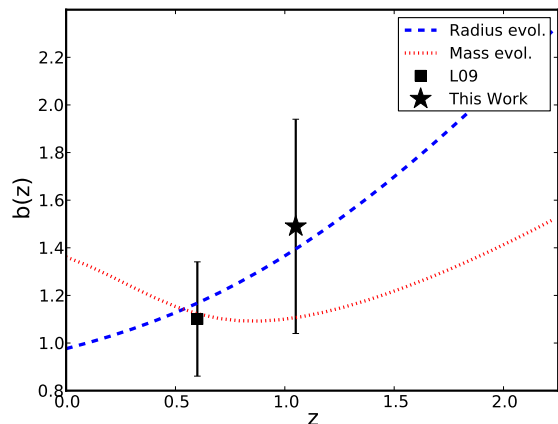


Figure 5. The bias of Mg II absorbers as a function of redshift. Model curves from Figure 3 in Tinker & Chen (2010) are overplotted, indicating the predicted bias of $W_r^{\lambda 2796} > 1.0 \text{ \AA}$ absorbers for separate models of evolving halo gas radius and mass. Bias measurements from Lundgren et al. (2009) and this work are overplotted, indicating a possible preference in the data for the scenario of evolving radius.

M_h . In doing so, they demonstrate that the observed anti-correlation of Mg II and bias at $z=0.6$ may be reproduced by the absence of high density cold gas in the hot haloes of the most massive (and most biased) galaxies.

Tinker & Chen (2010) built on the Tinker & Chen (2008) model to incorporate the observed redshift evolution of the Mg II number density, thus enabling predictions of the absorber halo occupation distribution as a function of redshift. The number density of Mg II absorbers in the SDSS has been shown to be roughly constant with redshift (Nestor et al. 2005; Prochter et al. 2006a; Lundgren et al. 2009). Reconciling this non-evolving Mg II number density within the context of hierarchical growth, which produces fewer haloes at a fixed mass at higher redshifts, requires evolution in the distribution of cold gas in haloes. One can achieve this effect by varying either the effective gas radius of the haloes or the typical absorber halo mass. As detailed in Tinker & Chen (2010), the observational outcomes of these two scenarios are degenerate in Mg II number density, but they diverge in predicted bias over a range in redshift.

In Figure 5 we overlay the Mg II bias measurement from this work onto the curves of projected bias evolution calculated separately for models of evolving gas radius and halo mass from Tinker & Chen (2010). The bias measurement at $z \sim 1$ suggests a preference for the model of gas radius evolution, though the error on our measurement is still too large to rule out the mass evolution model. It is important to note that the model curves of Tinker & Chen (2010) have been calculated for an absorber sample with $W_r > 1 \text{ \AA}$, whereas our data extends to a lower equivalent width limit. However, if the anti-correlation of bias and Mg II equivalent width holds, then we would expect our bias measurement to lie slightly above the generated curve, as it does. The amplitude of the disagreement between the model curves and our bias measurement may thus appear slightly exaggerated in this plot. Still, any correction due to the equivalent width

limit of the absorber sample is unlikely to change the measurement beyond the large, stated errors.

As detailed in Tinker & Chen (2010), the physical implications of a model without mass evolution require the gas radius of a halo, R_g , to expand relative to the halo virial radius, R_{200} , with increasing redshift as

$$R_g(M_h, z) = R_{200}(M_h) \times 0.4 \left(\frac{1+z}{1.6} \right)^{1.47}. \quad (6)$$

By this calculation, the gas radius should be just greater than half of the DM halo virial radius at $z=1$. This implies the gas radius increases by $\sim 40\%$ in units of R_{200} between $z=0.6$ and $z=1$.

The errors on our absorber bias measurement are largely due to the small number of Mg II absorbers available in this analysis. Thus, better constraining the absorber-galaxy cross-correlation measurement requires a deeper Mg II survey in the DEEP2 region. The size of the Mg II sample in this work is largely determined by the SNR and resolution of SDSS spectra. Follow-up observations of the same SDSS quasars with either higher SNR, higher resolution, or both might easily increase the number of Mg II detections, without necessitating the detection of many additional quasars within the survey footprint. Increasing the size of the DEEP2 Mg II data by a factor of 4, might reduce the error on the Mg II bias measurement sufficiently to rule out the Tinker et al. (2010) model of evolving halo mass.

A larger dataset may also enable measurements of bias for subsets of the absorber sample split by any number of observable parameters (e.g. equivalent width). Since previous analyses have identified a weak anti-correlation of absorber equivalent width and bias (Bouché et al. 2006; Lundgren et al. 2009; Gauthier et al. 2009), it would be interesting to examine whether any evolution in this trend is evident higher redshift. Due to the limitations of our current data, we must save this potentially interesting analysis for future work.

8.2 Comparison to Previous Measurements of the Mg II Covering Fraction

The average effective gas radius of $\sim 40 \text{ h}^{-1}\text{kpc}$, estimated from our measurement of the MgII covering fraction in DEEP2 galaxies, agrees well with the speculated extent of star-formation driven outflows from the same galaxy population, which was estimated by Weiner et al. (2009) to be $20\text{--}50 \text{ h}^{-1}\text{kpc}$.

Early studies found that galaxies with luminosities of $\sim L^*$ have a $W_r^{\lambda 2796} > 0.3\text{\AA}$ covering fraction of $0.25 \leq f_c \leq 1$ on scales less than $60 \text{ h}^{-1}\text{kpc}$ (Bergeron & Boissé 1991; Bechtold & Ellingson 1992; Steidel et al. 1994). These analyses revealed an anti-correlation between R_g and $W_r^{\lambda 2796}$, which was also shown to scale slightly with galaxy luminosity. An additional dependence of f_c and R_g on galaxy type was suggested by the results of Bowen et al. (1995), who used HST to examine $z < 0.2$ galaxies in close proximity to quasar sightlines. Bowen et al. (1995) measured an effective gas radius $R_g \sim 50 \text{ h}^{-1}\text{kpc}$ for galaxies with late-type or interacting morphologies and found an absence of Mg II absorption for the early-type galaxies with high confidence.

Due to the varying choices of galaxy samples, $W_{r,min}^{\lambda 2796}$, and median absorber redshift, the covering fraction mea-

surements from numerous other studies are difficult to directly compare with our results. Tripp & Bowen (2005) measured a covering fraction of $f_c \sim 0.5$ within $60 \text{ h}^{-1}\text{kpc}$ for $W_r^{\lambda 2796} > 0.1\text{\AA}$ absorbers at $z \sim 0.5$. Chen & Tinker (2008) measure a covering fraction of $f_c \sim 0.8$ within $69 \text{ h}^{-1}\text{kpc}$ for $W_r^{\lambda 2796} > 0.3\text{\AA}$, which seems to follow a scaling relation dependent on halo mass and galaxy luminosity. In general agreement with this result, Barton & Cooke (2009) measure $0.25 < f_c < 0.4$ for $W_r^{\lambda 2796} > 0.3\text{\AA}$ within $\sim 75 \text{ h}^{-1}\text{kpc}$ at $z \sim 0.1$.

A number of additional measurements, motivated by recent Mg II-LRG correlation results, have investigated the cold gas content of LRG haloes (Chen et al. 2010; Gauthier et al. 2010; Bowen & Chelouche 2011), which generally agree on a $W_r^{\lambda 2796} \geq 0.6\text{\AA}$ Mg II covering fraction of $\sim 10\%$ for $100 \text{ h}^{-1}\text{kpc}$ radii around LRGs. However, Bowen & Chelouche (2011) find little evidence to support a trend of decreasing f_c on the same scales with increasing galaxy luminosity, which might be expected if Mg II gas is evaporated at larger radii in the haloes of more luminous galaxies (Tinker & Chen 2008; Chen et al. 2010).

Unfortunately, the number of absorber-galaxy pairs at separations less than $100 \text{ h}^{-1}\text{kpc}$ in this work is insufficient to make a strong argument in support of any of these previous analyses. Future surveys to obtain quasar spectra with higher resolution and SNR would be most useful in order to better constrain the gas covering fraction of these galaxies. Such a dataset would also allow for the extension of the covering fraction measurement to lower absorber equivalent width limits.

9 SUMMARY

We measure the two-point cross-correlation function of 21 Mg II absorbers detected in the SDSS DR7 with $\sim 32,000$ spectroscopic galaxies from the DEEP2 galaxy survey in the redshift range $0.7 \leq z \leq 1.4$. By fitting models of the dark matter clustering to the results, we produce the first estimate of the dark matter bias and halo mass of Mg II absorbers at $z \sim 1$.

The bias we measure for the Mg II absorbers, $b_A = 1.49 \pm 0.45$, is consistent with that of the DEEP2 galaxy sample, $b_G = 1.44 \pm 0.02$. This finding suggests that strong ($W_r^{\lambda 2796} \gtrsim 0.6\text{\AA}$) Mg II absorbers occupy similar dark matter halo environments to those of the DEEP2 galaxies.

Haloes with the bias we measure for the Mg II absorbers have a corresponding mass of $1.8 \pm_{1.6}^{4.2} \times 10^{12} h^{-1} M_\odot$, although the actual mean absorber halo mass will depend precisely on how these absorbers populate DM haloes. In comparison with measurements at lower redshift, these results indicate that the dark matter halo masses of Mg II absorbers with $W_r^{\lambda 2796} \gtrsim 0.6\text{\AA}$ undergo no significant evolution from $z \sim 0.6$.

Since the redshift number density of these absorbers has also been shown to have roughly no evolution, these results agree with the Tinker et al. (2010) model in which only the gas radius of Mg II haloes evolves with redshift. Within this model, the gas radii of haloes expand with increasing redshift such that the haloes at $z=1$ have a gas radius that is $\sim 40\%$ larger in units of the DM halo virial radius, compared to $z=0.6$. However, the errors on our Mg II bias measurement

are still too large to rule out other halo evolution models in which the halo mass also evolves with redshift.

We measure the covering fraction of strong Mg II absorption to be $f_c=0.5$ within $60 \text{ h}^{-1}\text{kpc}$ around DEEP2 galaxies. We find no absorber host-galaxy pairs on scales larger than $37 \text{ h}^{-1}\text{kpc}$, suggesting that the effective gas radius of strong Mg II absorption around DEEP2 galaxies may be as small as $\sim 40 \text{ h}^{-1}\text{kpc}$.

In our sample, we identify just one candidate absorber host galaxy, which exhibits no evidence of ongoing star formation. Despite the small sample size, this finding suggests that absorbers with similar equivalent widths ($W_r^{\lambda 2796} \sim 1.8 \text{ \AA}$) may not preferentially trace galaxies with high star formation rates at $z \sim 1$. However, we stress that a much larger sample would be required to fully test this result.

A larger overlapping survey of quasars and galaxies will be necessary to better constrain measurements of the typical environments of Mg II absorbers as well as the cold gas covering fraction of typical galaxies at $z \gtrsim 1$. Surveys such as the SDSS-III Baryon Oscillation Spectroscopic Survey (BOSS), will soon provide the higher densities of quasars necessary to achieve this required precision. Follow-up spectroscopy of already identified quasars at higher resolution or signal-to-noise could additionally produce the numbers of absorbers in deep galaxy survey footprints needed to vastly improve our understanding of the distribution of cold gas in dark matter haloes in the near future.

ACKNOWLEDGMENTS

We would like to thank the referee, Jeremy Tinker, for helpful discussions and comments, which have greatly improved this work. We also thank JT for providing us with his model predictions, presented in Figure 5. We are also grateful to Pushpa Khare and Jean Quashnock for helpful discussions and to many others, who have contributed to the construction of the SDSS DR7 quasar absorption line catalog of York et al. (2011). Funding for the SDSS and SDSS-II has been provided by the Alfred P. Sloan Foundation, the U.S. Department of Energy, the National Aeronautics and Space Administration, the Japanese Monbukagakusho, the Max Planck Society, and the Higher Education Funding Council for England. The SDSS Web Site is <http://www.sdss.org/>.

REFERENCES

- Abazajian, K. N., et al. 2009, *ApJS*, 182, 543
- Adelberger, K. L., Shapley, A. E., Steidel, C. C., Pettini, M., Erb, D. K., & Reddy, N. A. 2005, *ApJ*, 629, 636
- Barton, E. J., & Cooke, J. 2009, *AJ*, 138, 1817
- Bechtold, J., & Ellingson, E. 1992, *ApJ*, 396, 20
- Bergeron, J. 1986, *A&A*, 155, L8
- Bergeron, J., & Boissé, P. 1991, *A&A*, 243, 344
- Blake, C., Collister, A., & Lahav, O. 2008, *MNRAS*, 385, 1257
- Bouché, N., Murphy, M. T., & Péroux, C. 2004, *MNRAS*, 354, L25
- Bouché, N., Gardner, J. P., Katz, N., Weinberg, D. H., Davé, R., & Lowenthal, J. D. 2005, *ApJ*, 628, 89
- Bouché, N., Murphy, M. T., Péroux, C., Csabai, I., & Wild, V. 2006, *MNRAS*, 371, 495
- Bouché, N., Murphy, M. T., Péroux, C., Davies, R., Eisenhauer, F., Förster Schreiber, N. M., & Tacconi, L. 2007, *ApJ*, 669, L5
- Bowen, D. V., Blades, J. C., & Pettini, M. 1995, *ApJ*, 448, 634
- Bowen, D. V., & Chelouche, D. 2011, *ApJ*, 727, 47
- Brown, M. J. I., Dey, A., Jannuzi, B. T., Lauer, T. R., Tiede, G. P., & Mikles, V. J. 2003, *ApJ*, 597, 225
- Brown, M. J. I., Dey, A., Jannuzi, B. T., Brand, K., Benson, A. J., Brodwin, M., Croton, D. J., & Eisenhardt, P. R. 2007, *ApJ*, 654, 858
- Brown, M. J. I., et al. 2008, *ApJ*, 682, 937
- Calder, M. A., Sheth, R. K., & Jain, B. 2010, *MNRAS*, 406, 1269
- Chelouche, D., & Bowen, D. V. 2010, *ApJ*, 722, 1821
- Chen, H.-W., & Tinker, J. L. 2008, *ApJ*, 687, 745
- Chen, H.-W., Helsby, J. E., Gauthier, J.-R., Shectman, S. A., Thompson, I. B., & Tinker, J. L. 2010, *ApJ*, 714, 1521
- Coil, A. L., et al. 2004, *ApJ*, 609, 525
- Coil, A. L., Newman, J. A., Kaiser, N., Davis, M., Ma, C.-P., Kocevski, D. D., & Koo, D. C. 2004, *ApJ*, 617, 765
- Coil, A. L., Hennawi, J. F., Newman, J. A., Cooper, M. C., & Davis, M. 2007, *ApJ*, 654, 115
- Cool, R. J., et al. 2008, *ApJ*, 682, 919
- Cristiani, S., Danziger, I. J., & Shaver, P. A. 1987, *MNRAS*, 227, 639
- Chun, M. R., Kulkarni, V. P., Gharanfoli, S., & Takamiya, M. 2010, *AJ*, 139, 296
- Davis, M., et al. 2003, *Proc. SPIE*, 4834, 161
- Eisenstein, D. J., Blanton, M., Zehavi, I., Bahcall, N., Brinkmann, J., Loveday, J., Meiksin, A., & Schneider, D. 2005, *ApJ*, 619, 178
- Faber, S. M., et al. 2003, *Proc. SPIE*, 4841, 1657
- Gauthier, J.-R., Chen, H.-W., & Tinker, J. L. 2009, *ApJ*, 702, 50
- Gauthier, J.-R., Chen, H.-W., & Tinker, J. L. 2010, *ApJ*, 716, 1263
- Hawkins, E., et al. 2003, *MNRAS*, 346, 781311
- Helene, O. 1984, *Nuclear Instruments and Methods in Physics Research A*, 228, 120
- Kacprzak, G. G., Churchill, C. W., Ceverino, D., Steidel, C. C., Klypin, A., & Murphy, M. T. 2010, *ApJ*, 711, 533
- Kacprzak, G. G., Churchill, C. W., Barton, E. J., & Cooke, J. 2011, *arXiv:1102.4339*
- Kaiser, N. 1987, *MNRAS*, 227, 1
- Le Brun, V., Bergeron, J., Boisse, P., & Christian, C. 1993, *A&A*, 279, 33
- Landy, S. D., & Szalay, A. S. 1993, *ApJ*, 412, 64
- Lundgren, B. F., et al. 2009, *ApJ*, 698, 819
- Meiring, J. D., Lauroesch, J. T., Haberbacht, L., Kulkarni, V. P., Péroux, C., Khare, P., & York, D. G. 2011, *MNRAS*, 410, 2516
- Ménard, B., Wild, V., Nestor, D., Quider, A., & Zibetti, S. 2009, *arXiv:0912.3263*
- Ménard, B., & Chelouche, D. 2009, *MNRAS*, 393, 808
- Ménard, B., Wild, V., Nestor, D., Quider, A., & Zibetti, S. 2009, *arXiv:0912.3263*
- Nestor, D. B., Turnshek, D. A., & Rao, S. M. 2005, *ApJ*, 628, 637

- Nestor, D. B., Turnshek, D. A., Rao, S. M., & Quider, A. M. 2007, *ApJ*, 658, 185
- Nestor, D. B., Johnson, B. D., Wild, V., Ménard, B., Turnshek, D. A., Rao, S., & Pettini, M. 2010, arXiv:1003.0693
- Noterdaeme, P., Srianand, R., & Mohan, V. 2010, *MNRAS*, 403, 906
- Padmanabhan, N., White, M., Norberg, P., & Porciani, C. 2009, *MNRAS*, 397, 1862
- Prochter, G. E., Prochaska, J. X., & Burles, S. M. 2006, *ApJ*, 639, 766
- Ross, N. P., et al. 2007, *MNRAS*, 381, 573
- Schiavon, R. P., et al. 2006, *ApJ*, 651, L93
- Schneider, D. P., et al. 2010, *AJ*, 139, 2360
- Smith, R. E., et al. 2003, *MNRAS*, 341, 1311
- Straka, L. A., Kulkarni, V. P., York, D. G., Woodgate, B. E., & Grady, C. A. 2010, *AJ*, 139, 1144
- Steidel, C. C. 1993, *The Environment and Evolution of Galaxies*, 188, 263
- Steidel, C. C., Dickinson, M., & Persson, S. E. 1994, *ApJ*, 437, L75
- Steidel, C. C., Dickinson, M., Meyer, D. M., Adelberger, K. L., & Sembach, K. R. 1997, *ApJ*, 480, 568
- Tinker, J. L., Weinberg, D. H., Zheng, Z., & Zehavi, I. 2005, *ApJ*, 631, 41
- Tinker, J. L., Weinberg, D. H., & Zheng, Z. 2006, *MNRAS*, 368, 85
- Tinker, J. L., & Chen, H.-W. 2008, *ApJ*, 679, 1218
- Tinker, J. L., Robertson, B. E., Kravtsov, A. V., Klypin, A., Warren, M. S., Yepes, G., & Gottlöber, S. 2010, *ApJ*, 724, 878
- Tinker, J. L., & Chen, H.-W. 2010, *ApJ*, 709, 1
- Tripp, T. M., & Bowen, D. V. 2005, *IAU Colloq. 199: Probing Galaxies through Quasar Absorption Lines*, 5
- Wake, D. A., et al. 2006, *MNRAS*, 372, 537
- Wake, D. A., et al. 2008, *MNRAS*, 387, 1045
- Wake, D. A., Croom, S. M., Sadler, E. M., & Johnston, H. M. 2008, *MNRAS*, 391, 1674
- Wake, D. A., et al. 2011, *ApJ*, 728, 46
- Weiner, B. J., et al. 2009, *ApJ*, 692, 187
- Wild, V., Hewett, P. C., & Pettini, M. 2007, *MNRAS*, 374, 292
- Wild, V., et al. 2008, *MNRAS*, 388, 227
- Yanny, B., York, D. G., Hamilton, D., Schommer, R. A., & Williams, T. V. 1987, *ApJ*, 323, L19
- York, D. G., et al. 2000, *AJ*, 120, 1579
- York, D. G., et al. 2006, *MNRAS*, 367, 945
- York, D. G., et al. 2011, in preparation.
- Zehavi, I., et al. 2005, *ApJ*, 621, 22
- Zheng, Z., et al. 2005, *ApJ*, 633, 791
- Zibetti, S., Ménard, B., Nestor, D. B., Quider, A. M., Rao, S. M., & Turnshek, D. A. 2007, *ApJ*, 658, 161

Table 1. Mg II Absorption Line Data

ID	RA	Dec	z_{QSO}	m_i	$z_{Mg II}$	$W_r^{\lambda 2796}(\text{\AA})$	$W_r^{\lambda 2803}(\text{\AA})$
1	351.487322	-0.083341	1.4082	18.64	0.9432	0.8301 ± 0.1817	0.8980 ± 0.2115
2a	351.894734	0.376114	1.4939	18.12	0.9530	0.7624 ± 0.1132	0.5218 ± 0.0942
2b	1.3378	0.5715 ± 0.1120	0.3760 ± 0.1035
3	352.190154	0.083659	1.5272	19.20	0.9575	0.7678 ± 0.1819	0.9195 ± 0.2830
4	353.117552	0.009120	1.6039	18.37	0.8301	0.9497 ± 0.1339	0.4552 ± 0.0820
5	351.848711	-0.045322	1.2276	19.85	0.8184	1.3990 ± 0.2354	0.8161 ± 0.2398
6	37.391944	0.756865	1.8999	20.04	1.3018	2.4576 ± 0.2789	1.6670 ± 0.2828
7	252.786865	34.942695	1.5404	18.17	1.2706	2.0955 ± 0.1149	1.9330 ± 0.1440
8a	252.792496	35.086504	2.2455	19.78	0.8715	0.8865 ± 0.2100	1.0649 ± 0.1892
8b	0.8765	1.0621 ± 0.1886	0.7157 ± 0.1913
9	36.928474	0.667494	1.8943	19.48	1.3302	1.4213 ± 0.2219	1.1321 ± 0.2459
10	36.875592	0.792676	1.4858	19.75	0.7751	1.9954 ± 0.4050	1.0501 ± 0.2772
11a	214.659800	52.399823	1.1181	18.68	0.7236	0.5651 ± 0.1213	0.5071 ± 0.1445
11b	1.0227	1.5198 ± 0.1661	0.9206 ± 0.1256
12	215.023321	53.010203	1.6467	19.79	1.3172	1.3978 ± 0.3068	0.7815 ± 0.1964
13	252.112461	35.004821	2.9356	19.08	1.2803	0.8275 ± 0.1004	0.7407 ± 0.1723
14	351.815063	0.237062	2.5291	20.00	1.0394	2.0403 ± 0.4246	3.2598 ± 0.4487
15	351.644600	0.363794	1.2571	20.24	0.7459	1.7217 ± 0.3797	1.3855 ± 0.3918
16	37.002673	0.453234	2.3975	19.61	0.7219	1.7812 ± 0.1318	1.3863 ± 0.1208
17	36.683492	0.551612	2.3761	19.90	1.3523	0.5641 ± 0.1105	0.3256 ± 0.0799
18	36.790855	0.461854	2.3879	20.89	1.2268	1.4689 ± 0.2991	0.9484 ± 0.3121